COBEM 2023 27TH INTERNATIONAL CONGRESS OF MECHANICAL ENGENEERING

ABCM Brazilian Society of Mechanical Sciences and Engineering
27th ABCM International Congress of Mechanical Engineering
December 04-08, 2023, Florianópolis-SC, Brazil

# COB-2023-0691
# A RENEWED CONTEMPORARY ANALYSIS OF CHIP FORMATION FREQUENCY ON LATHE OPERATION OF SAE 4340 ROLLED BAR UNDER DIFFERENT REMOVAL RATE CONDITIONS

**Marcelo Acacio De Luca Rodrigues**
Vila Companhia Fabricadora de Skate
marcelo.lean.engenharia@gmail.com

**Bruno Fernandes de Holanda**
Saneamento Básico do Estado de São Paulo - SABESP
Fernandes.holanda@hotmail.com

***Abstract.*** *This article aims to describe a simple analysis of chip formation frequency at machining lathe operation based on the measured and calculated metal removal rate and the theoretical velocity diagram under some variations of cutting speed. This investigation is a subject presented on manufacturing process classroom of Production and Mechanical engineering courses and all the detailed mathematical and physical modeling is accomplished by the students on a mixed of theoretical and practical class. The collected results consider classical physics from the continuity equation to describe a technological concept within machining science and it helped the students to understand both aspects. The continuity equation became easier when applied on a technological matter with this method of analysis and measurement of the mass flow on the chip formation. In the same way the technical details of the machining operation helped the comprehension of advanced topics usually restricted to advanced solid mechanics and plasticity courses. The velocity diagrams were defined after the mass measurement and they are in total agreement with chip formation theory. The very stable chip shape supported the idea of average chip mass for each cutting speed. A difference between measured and calculated removal rate was found and it is justified by the undefined shear plane direction however the classical suggestion for this value solves the set of equation according to the classical Shawn and Kronenberg´s graphs.*

.

***Keywords:*** *Metal removal rate, chip frequency formation, velocity diagram, continuity equation, mass balance*

## 1. INTRODUCTION

The metal removal rate is the first efficiency parameter that indicates whether a cutting condition is better than another regardless of the unavoidable wear that occurs during the machining operation. A faster metal removal rate indicates that chip formation is faster. In other words, the frequency for the chip flow and the frequency for the strain rate that takes place during the machining is faster. These two phenomena take place simultaneously thus the frequency of the chip formation leads to the idea of metal removal rate, but its complexity is not simply solved by the metal removal equation.

A classic velocity diagram (Merchant, 1945; Shawn, 1966; Kronemberg, 1967; Stephenson et al., 2016) for chip formation is reproduced in most of the contemporary literature about machining without a reasonable discussion (Astakhov, 1998) or even a suitable set of results to illustrate the geometrical relation among cutting speed ($v_c$), shear velocity ($v_s$) and chip velocity ($v_{ch}$). All the contemporary authors emphasize the same equations for the velocity diagram except Zorev (1966).

The continuity equation that is classically applied on the forming process also can be used to support the idea of mass balance of the open thermomechanical machining system. It means that a machining system described as an exothermic open thermodynamic system must be in agreement with the continuity of mass (Stephenson et al., 2016; Stahl, 2012). The conservation of mass on the machining system is an initial condition to support the velocity diagram. Astakhov (2001) suggests a new interpretation of the velocity diagram based on the three stages chip formation description which includes the unavoidable discontinuity along and nearby the shear plane as a possible solution for velocity diagram.

It was observed during this investigation a lack of recent articles which discuss the metal removed rate related with the velocity diagram.

A lathe cylindrical external machining operation of a well-known SAE 4340 steel was conducted to initiate this discussion considering the continuity equation for metal flow but in this case with chip formation. The metal removal rate was manipulated and the chip flow frequency was discussed.

A very simple experiment which considers the mass reduction on the machined specimen among every trial indicated that the initial velocity has a direct relation with the chip flow despite the chip compression factor but finally, considering mass continuity on the system, the initial velocity is the same on scalar magnitude as the chip velocity for producing the same MRR.

This investigation is a compilation of several laboratory classes of machining process to perform the concept of productivity based on the metal (or material) removal rate and how the velocity diagram takes places during the chip formation. Specific concepts related to materials' behavior such as strain hardening or the influence of heat treatment or chemical composition are not focused on this discussion. So, the wear is not considered as it is explained in section 3 in fact. The effect of the wear is only cited on the classroom for this topic. Further activities must complete the idea of productivity considering the wear and some other quality aspects directly obtained from the machining process such as the surface roughness. Students are confident in evaluating the metal removal rate after this laboratory approach.

No intention to disregard the foundation of the velocity diagram is expressed in this investigation. Original Figures from the Kronenberg (1966) and Shaw (1965) were kept in order to respect them masterpieces and also to teach the students to study and investigate using the original sources.

## 2. BIBLIOGRAPHIC REVIEW

There are several mechanical and metallurgical engineering topics related to the following sections. However, the main aspects that are possible to be discussed on graduate courses are detailed bellow.

### 2.1 Metal removal rate for lathe operation

The metal removal rate (*MRR*) is the amount of material cut from the raw workpiece material from previous operation in a time interval. Every tool manufacturer manual, handbook, leaflet, brochure or presentation indicates the Eq. (1) to obtain this value for lathe operation. Figure 1 illustrates Eq. (1) for lathe operation performing cylindrical external turning. $Ac$ ($m^2$) is the cutting area, $v_c$ is the cutting speed (m/min), $a_p$ is cutting depth (m), $f_c$ is the feed per revolution (m/rev).

$$\dot{Q} = MRR = A_c . v_c = a_p . f_c . v_c \tag{1}$$

The *MRR* can be understood as the result of the cutting speed times the cutting area. It's important to consider some geometrical details such as lead angle, the rake angle and clearance angle to define the correct cutting area as seen at Figure 1.

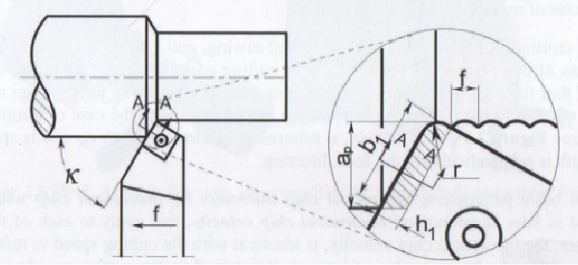


Figure 1 – The cutting area, adapted from Stahl (2012)

The corner radius r (m) is also important to define this area. The cutting speed and feed per revolution are combined with the major cutting angle $\kappa$ (deg) to produce the same *MRR* with different chip shapes. Every time the major cutting angle $\kappa$ changes, the cutting area remains the same but the chip width $h_1$ (m) and chip length $b_1$ (m) change, producing a different chip cross section with a different flowing direction but finally the same *MRR*. It is usual that tangential velocity is considered constant in Eq. (2) on cylindrical external turning. An angular speed $\omega$ (rad/s) is sometimes more convenient to be related to the chip flow in Eq. (3). An exciter frequency $f$ (Hz) raises initially from the cutting speed in Eq. (4). $\emptyset$ (m) is the considered diameter for obtaining the cutting speed and the exciter frequency.

$$Vc = \frac{\pi . \emptyset . n}{1000} \tag{2}$$

$$\omega = \frac{2 . v_c}{\emptyset} \tag{3}$$

$$f = \frac{\omega}{2\pi} \tag{4}$$

On a very brief discussion about the exciter frequency (*f*), it is the primary frequency of the system when observed by the vibrational spectrum. This is the frequency related with the rotational parameter (n). It is not the frequency of the chip formation because no relation is seen between the exciter frequency and the rate of the chip that leaves the cutting system.

### 2.2 Velocity diagram on chip formation

It's easy to identify on the machining literature that the velocity diagram is widespread the same (Asthakov, 1998). Only a few details are presented on several literature references to describe the three components of the diagram. Kronenberg (1966) and Shawn (1965) have approached the relations around the velocity diagram regarding the influence of chip compression ratio $\lambda_h$ (dimensionless) and an also a graphical definition of the share angle $\phi$ (deg.). Kronenberg (1966) brightly illustrates the velocity diagram as shown in Figure 2, and from the same Kronenberg masterpiece chip compression factor can assume the unity as a possible value.

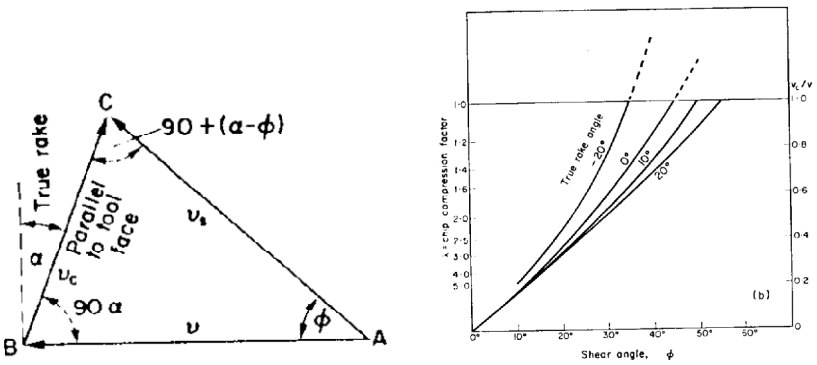


Figure 2 – Fundamental definition of the shear angle and chip compression factor, adapted from Kronenberg (1966).

The definition of the shear angle leads to the solution of the velocity diagram, where the sine law between the cutting velocity and chip velocity results on shear velocity. Once the shear angle is difficult to be measured, a range of angles can be considered for the solution of Eq. (5) up to Eq. (8). The assumptions of a range of angles is the base for the nomographs classically presented by Shawn (1965) which relates both the shear angle and the chip compression factor as a function of the rake angle Shaw (1965) and Kronenberg (1966) are in total agreement.

Astakhov (1999) considers some models to explain the problems around the definition of the velocity diagram. The main problem is focused on the mathematical limit of the shear velocity regarding the possibility of applying a neutral rake angle tool which affects the shear angle.

Classical kinematics defines the velocity diagram in terms of linear velocity. However. The cheap formation has a frequency, so it is cyclical, (Astakhov, 1999). The chip formation has a classical description for it to occur with some corrections between ductile or fragile materials. Equations (2), (6) and (7) present the velocity elements of the diagram and Eq. (5) presents the chip compression factor.

$$\lambda_h = \frac{h_2}{h_1} \tag{5}$$

Figure 3 adapted from Stahl (2012) illustrates the terms for the Eq. (5) up to Eq. (8) while Figure 2 demonstrates the rake angle. It is very important to consider that by the time when the Eq. (5) up to Eq. (8) were developed the rake angle could be manipulated but not as simply as today´s technology for the tool assembly. So, to consider a correct rake angle $\alpha$ (deg.) it is necessary to identify the tool rake incidence connection and the chip breaker detail in terms of the feed per revolution *f*' (m/rot).

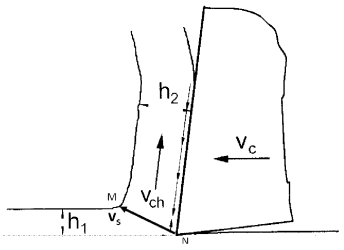


Figure 3 – Definition of the cutting system related to the chip compression factor.

$$v_{ch} = \frac{sen\phi}{\cos(\phi - \alpha)} . v_c = \frac{v_c}{\lambda_h} \tag{6}$$

$$v_s = \frac{\cos\alpha}{\cos(\phi - \alpha)} . v_c \tag{7}$$

$$\tan\phi = \frac{\cos\alpha}{(\lambda_h - sen\alpha)} \tag{8}$$

According to Eq. (6) up to Eq. (8), the $\phi$ is the shear angle which defines the shear plane MN at Figure 3. $\alpha$ is the effective rake angle and $\lambda_h$ is the chip compression factor.

### 2.3 Frequency and strain rate on chip formation

The frequency of the chip formation is divided into two aspects: chip flow frequency and strain rate.

Shaw presents in his first edition manuscript (1965) a reliable and didactic description of the shear plane detail which helps strictly to understand strain rate $\dot{\gamma}$ based on the shear velocity. Shawn and Merchant (1945) converge with Figure 4 and Eq. (9) and Eq. (10). The simple concept of strain rate considers that a constant undeformed volume of material gets across the shear plane during a very sensible period. The only strain effect is shear (Shawn, 1965). And this effect is a consequence of compression. This very simple model based on the Shawn (1965) description has a very difficult detail to be defined to resume the chip formation: the distance between the parallel shear plane Δy. Shawn´s representation emerges from the very classic cards model from Pisspanen foundation system for continuous chip (Merchant, 1945; Piispanen, 1948). Once this distance is not measured, Eq. (10) may be solved for a considered range of shear plane distance Δy which satisfies the continuity and other aspects around the mechanism.

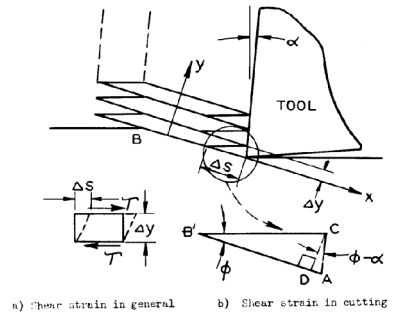


Figure 4 – Determination of the shear strain $\dot{\gamma}$ in cutting, adapted from Shawn (1965).

$$\gamma = \frac{\cos\alpha}{sen\alpha . cos(\phi - \alpha)} \tag{9}$$

$$\dot{\gamma} = \frac{\Delta S}{\Delta y . \Delta t} = \frac{V_S}{\Delta y} = \frac{\cos\alpha}{\cos(\phi - \alpha)} \frac{v_c}{\Delta y} \tag{10}$$

Cutting is supposed to occur after a shear stress γ exceeds a certain value that no longer the material can support it on the plastic field of strain. Plastic strain occurs and as soon as the critical value of separation is reached, the material is cyclic cut apart. And this description may lead to the separation in one single set of slip, or many slips must take place to indicate that a chip is formed and despite some mechanical factors such as bending, shrinkage, strain hardening,

the material is cut. The combinations of dynamic factors, geometric details of the cutting tool added to materials behavior result in the amount of slip that is usually characterized as the internal side of the chip. The very narrow profile of the internal side of the chip is an idealization in fact, and accord to the Astakov (1999), it is never mentioned how far this idealization deviates from reality.

### 2.4 Continuity equation on metal flow

The continuity equation is always presented on graduated course in energy topics such as fluid mechanics or even thermodynamics. Subjects related to metal forming are about to discuss the mass flow to obtain a certain profile using specific dynamic forming technology (press, mould and die, puncher, extruders, etc).

The cyclical consideration of the chip formation may be understood as a mass flow system problem. The chip formation divided into chip flow and strain rate demonstrates that some important relations of continuity is the same even with the desirable separation that occurs on machining.

Machining process has separation. It means that two bodies become three in an open thermodynamic system. The raw material is processed and the chip mass flows outside with a reasonable amount of converted energy.

One important contribution of thermodynamics to the machining process is the idea of energy equilibrium based on the change of mechanical energy into heat and strain.

It's common to observe at the machine shop or even at graduate laboratory class that the amount of mass is sometimes measured by any reason or another. But it's not taken as important information to model the process. However, considering the continuity of the mass even with the separation, the amount of mass of the system is the same before and after the machining process. There are some special machining processes which this balance can't be constant. Lathe operation under regular cutting speed without chip fusion can consider the mass before and after the same. No mass disappears. And no extra mass gets into the system. An open thermodynamic system has a function to describe how the mass changes.

An important consideration about the mass continuity, even with the separation, is the change of form. The density of the material is the same before and after the machining process. A chip has a very particular shape among several manufacturing processes with separation because of its cyclic mechanism. A packing factor indicates whether a good chip or a bad chip is produced and leaves the cutting area (Stephenson et al., 2016). The Eq. (11) is the synthesis of the continuity equation when the flow before the process is $\dot{Q}_1$ and the flow after is $\dot{Q}_2$. $V_1$ and $V_2$ are the mass volume, $m_1$ and $m_2$ are the masses (Kg) and $L_1$ and $L_2$ are the length (m). A unitary chip volume $\boldsymbol{V_{ch}}$ ($m^3$) on Eq. (12) can be obtained by the ratio between the unitary mass $m_{ch}$ (Kg) and the material´s density $\rho$ ($Kg/m^3$).

$$\dot{Q}_1 = \dot{Q}_2 \;\therefore\; \frac{V_1.m_1}{L_1} = \frac{V_2.m_2}{L_2} \tag{11}$$

$$\boldsymbol{V_{ch}} = \frac{m_{ch}}{\rho} \tag{12}$$

### 2.5 Mass measurement on machining

A very simple interpretation of the removed material on cylindrical lathe operation begins with the tool engagement distance $e_T$ (m) (Stahl, 2012). $t_c$ is the cutting time and $Lc$ is the cutting length (m). This quantity is the spiral distance covered by a cutting edge with constant feed and cutting speed. $f'$ is the feed per revolution.

$$e_T = v_c.t_c = \frac{L_c}{f'} \tag{13}$$

An idealized unitary chip volume $\boldsymbol{V_{ch}}$ has the following definition according to Eq. (12) up to Eq. (14). Figure 5 demonstrates this idealized volume. The $L_{ch}$ the unitary chip height. Once the Eq. (10) and Eq. (14) are easily solved with a reasonable unitary mass measurement, the $h_2$ is obtained.

$$\boldsymbol{V_{ch}} = \frac{a_p}{\text{sen}\kappa}.h_2.L_{ch} = b_1.h_2.L_{ch} \tag{14}$$

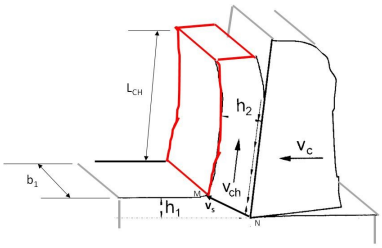


Figure 5 – Idealized unitary chip volume

Thus the total removed mass $m_t$ and a unitary chip mass $m_{ch}$ are measured, it is possible to suppose the numbers unitary chip removed them the ratio ($N_{ch} = m_t/m_{ch}$).

$$L_{ch} = \frac{e_T}{\left(\frac{m_t}{m_{ch}}\right)} \tag{15}$$

Therefore, a chip flow frequency $f_{ch}$ (Hz) can be estimated according to Eq. (16). The $t_c$ (s) is the effective cutting time to remove the quantity $N_{ch}$ of unitary chips.

$$f_{ch} = \frac{N_{ch}}{t_c} \tag{16}$$

As it can be seen on Figure 5, the internal side of the chip is not serrated as it use to be discussed. However there are many combinations of dynamic cutting conditions and metallurgical behavior that leads to a not serrated internal side. Nevertheless, even when a continuous strip is cut the result is still a chip with a very low chip flow frequency.

## 3. EXPERIMENTAL PROCEDURE

The goal of this investigation is to evaluate the chip flow frequency and the MRR measured and calculated during the cylindrical external lathe operation. The velocity diagram, the shear angle estimative and the continuity equation approach are the breakthrough of this investigation. The chip compression factor is one of the idealized result that consolidates the significance of this study.

### 3.1 Materials and equipments

The experimental set up is described below.

*Machine:* Universal turning lathe Nodus 220, 5 CV Power. Gear box driver and feed control.

*Specimen*: Cylindrical workpiece of SAE bar rolled 4340, hardness 240 HB. Initial total length is 0,278m. Initial diameter is 0,070m. Initial mass is 6,813Kg with coefficient of variation equals 0,8%. The density considered is 7900 $Kg/m^3$.

*Cutting tool:* CNMG 120408 PM 4225 insert and a PCLNR 2020 K12 tool holder. The total rake angle offered by this assemblage is 0° (insert is 5° and tool holder is -5°).

*Cutting fluid:* dry machining.

*Measurement*: a digital precision mass scale Marte Classe II 0 to 0,500Kg, division of 0,1g and error of 0,01g. A digital mass scale 0 to 10Kg, division of 1g and error of 1g. An analogic caliper rule 0 to 0,150m. A graduated mass scale 0 to 0,300m.

Devices: Chip collector, three points jaw with a rotative workpiece holder.

The sample was fixed on the lathe according to Figure 6. The tool holder was fixed with standard position providing $\kappa = 95°$.

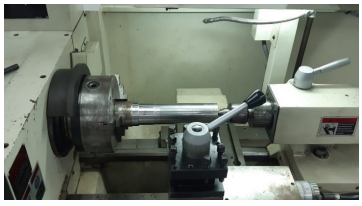

Figure 6 – Experimental set up.

### 3.2 Experimental Proceedure

The experimental procedure according to Tab.1 performed seven trials with different rotational speed ($n$) which resulted in seven different cutting speeds ($v_c$). The theoretical feed per revolution ($f'$) was fixed in 0,3m/rev. The theoretical cutting depth ($a_p$) was 1,5m. The operational procedure to each trial is described below:

a. Select the gear set for the rotational speed and feed per revolution;
b. Set the diameter reference to achieve the desired cutting depth;
c. Do the machining and collect as more chip as possible with the chip collector. Measure and write down the effective cutting time;
d. Wait for the chip to get cold and measure 3 samples of 10 chips per each sample.
e. Measure and write down the cutting length;
f. Photograph the chip, discard the chip, measure the diameter and start a new trial;

The Figure 7 illustrates the routine performed.

Figure 7 – Experimental set up.

## 4. RESULTS & DISCUSSION

Table 1 and the following graphs are obtained from the execution of the experimental planning (see sections 3.1 and 3.2). The Table 1 presents the values of MRR calculated and measured.

Table 1 – Experimental planning and results (resumed).

| *Trial* | *Initial mass (g)* | *Rotational speed (rpm)* | *Cutting speed (m/min)* | *Feed (mm/min)* | *Effective feed per revolution (mm/rev)* | *Calculated MRR ($cm^3$/min)* | *Measured MRR ($cm^3$/min)* |
|---|---|---|---|---|---|---|---|
| 7 | 6157 | 300 | 52,31 | 95,015 | 0,317 | 30,648 | 34,045 |
| 6 | 6255 | 475 | 83,42 | 168,297 | 0,354 | 48,767 | 48,552 |
| 2 | 6698 | 600 | 115,55 | 226,394 | 0,377 | 65,398 | 67,056 |
| 5 | 6365 | 750 | 134,77 | 282,090 | 0,376 | 53,226 | 51,820 |
| 4 | 6442 | 950 | 168,33 | 334,746 | 0,352 | 86,003 | 82,600 |
| 1 | 6814 | 950 | 192,11 | 345,378 | 0,364 | 105,813 | 106,372 |
| 3 | 6540 | 1500 | 264,37 | 525,000 | 0,350 | 148,044 | 145,372 |

Figure 7 presents the unitary chip mass as a function of the cutting speed. The faster the machining process the smaller is the chip. A cutting speed of 52,31 m/min indicates an unitary chip mass of 0,091g. A cutting speed of 264,37 m/min indicates an unitary chip mass of 0,037g. It is a regular result because a solution to decrease the chip size on machining can be the increase of the cutting speed. The coefficient of variation of the unitary chip mass was less than 1%. It justifies the number of 10 chips taken three times randomly to derive the average unitary chip mass. In other words the chip form was plainly stable to every cutting speed.

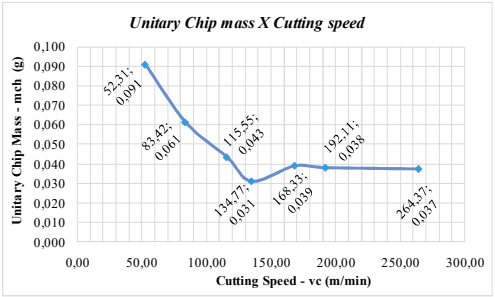


Figure 7 – Unitary chip mass as a function of the cutting speed.

Figure 8 presents the exciter frequency (or the primary frequency) obtained from the cutting speed on a specific diameter. Eq. (16) is the chip flow frequency. The chip flow frequency is higher that the exciter because the number of chip in a single round is much higher than a unity. At the limit it would the same if the chip was a unbroken strip.

The chip flow frequency is the ideal frequency obtained from the number of chip removed in one trial.

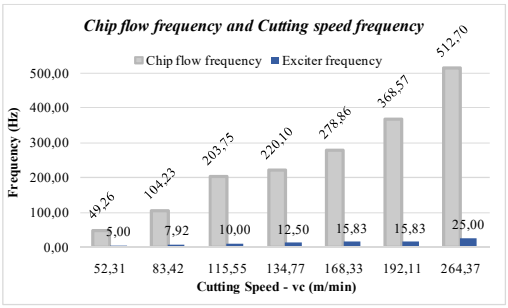


Figure 8 – Chip flow frequency and the primary frequency of the machining system.

Figure 9 is a comparison between the chip thicknesses. The deformed chip has a higher cross section at lower cutting speed. The $h_2$ decreases with the cutting speed and by the time the shear angle ($\phi$) is 45° and the rake angle is zero, the $h_2$ becomes less than $h_1$. The $h_1$ is a function of the actual feed per revolution combined with the $\kappa$ ($h_1 = f'.\sin\kappa$). At the machine shop, regarding the competence and experience to manage with the chip logistic, the higher cutting speed indicates such a perfect chip and even the qualitative result of the roughness and even the sound is greater at higher cutting speed. The $h_2$ was calculated according to Eq. (14) and Eq. (16) and its not controversial consider a lower $h_2$ than $h_1$ when the material is fragile.

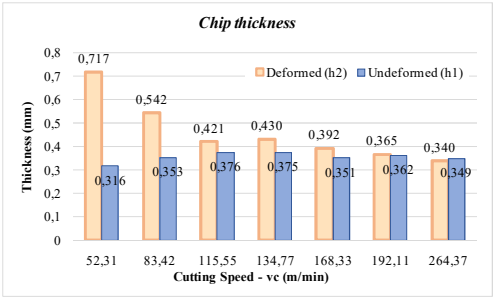


Figure 9 – The ratio between $h_2$ and $h_1$ indicates the chip compression factor.

The graphs on Figure 10 are the same but the interesting possibility is to compare the chip compression factor with the cutting speed and the shear angle simultaneously. The cutting speed of 52,31 m/min indicates the shear angle of 23,84°. The cutting speed of 264,37 m/min indicates the shear angle of 45,83°. The chip compression factor of 0,971 is justified the chip with higher frequency and lower strain. The graph on the left may suggest the use of Figure 2 presented by Kronenberg (1966) once the rake angle is known or not. The Figure 10 materializes the use of Figure 2 and a sequence of other brilliant theoretical deduction from Kronenberg's and Shaws masterpiece.

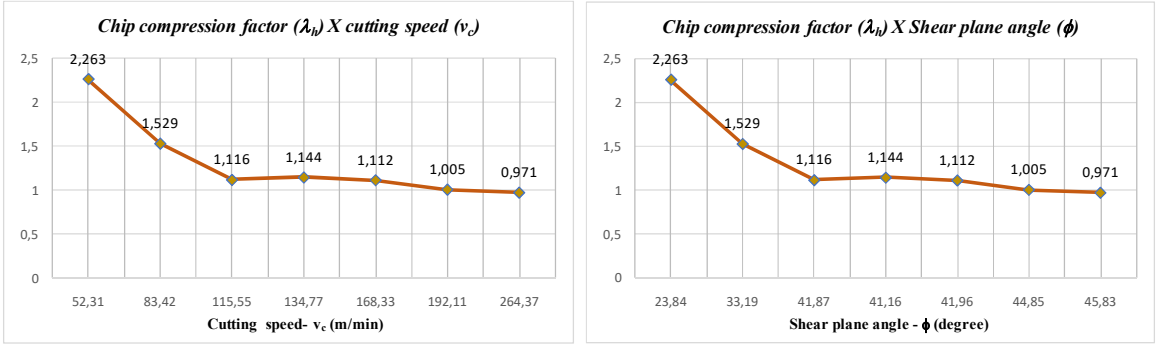


Figure 10 – The horizontal axes are different and shall be combined to conclude the $\lambda_h$.

The comparison of MRR presented on Figure 11 converges and all the differences between the two bars are justified by experimental errors. The measured MRR is the simplest application of the continuity equation (the ratio between the total removed mass by the cutting time) and the calculated MRR is obtained by Eq. (1). Even though the chip flow frequency is directly related with the direction of the flow which leads to the MRR, the cutting speed is still considered as the energy input and the convergence between the bars on Figure 11 is only possible with that value instead of the chip velocity. The measured bars are related with the time measurement which little distrortion emerges from it.

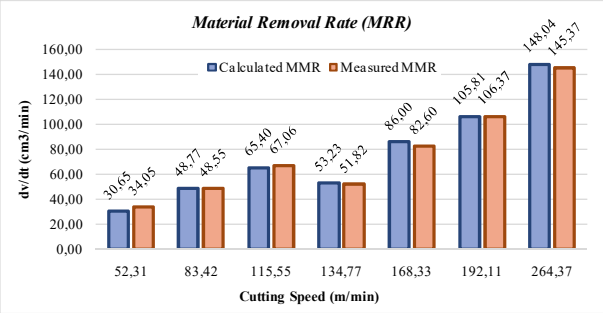


Figure 11 – Strict convergence between the two methods for measuring the MRR.

Figure 12 can be plotted once the values of cutting speed ($v_c$), shear angle ($\phi$), chip compression factor ($\lambda_h$) and rake angle ($\alpha$) are known, the Figure 12. The last bar is impossible considering the physical distribution of the kinematics among the three velocities on the diagram, by the other hand it is a possible result when the shear angle is higher than 45° with a zero rake angle.

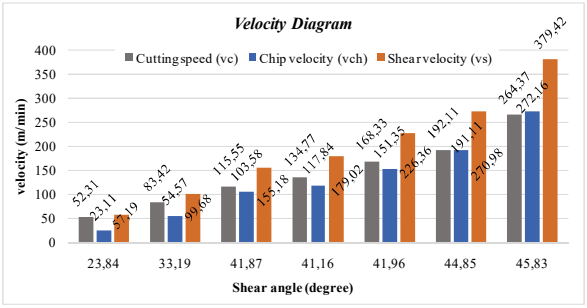


Figure 12 – The base values for the velocity diagram.

The velocity diagrams based on the values of Figure 12 are presented on Figure 13. It is a remarkable contribution of this humble investigation to the velocity diagram theory once it is not found on the literature cited and further. The velocity diagrams plotted are the demonstration of the idealized Figure 2 (Kronenberg, 1966). The impossible composition of the velocity diagram, remarked by Astakhov (1999) is easily seen. At the same Figure 2, it is possible to observe one milestone truth: the chip velocity is parallel to the rake face. The rake angle is zero so the chip velocity must orthogonal to the cutting speed direction. The blue arrow on Figure 13 was taken as a result of the intersection between two circles with $v_s$ and $v_{ch}$ as the radius of them. It is directly seen that chip velocity is orthogonal to the cutting speed. Thus, to all the trials, the shear velocity becomes a hypotenuse and it is greater that the cutting speed which is an adjacent of the same right triangle.

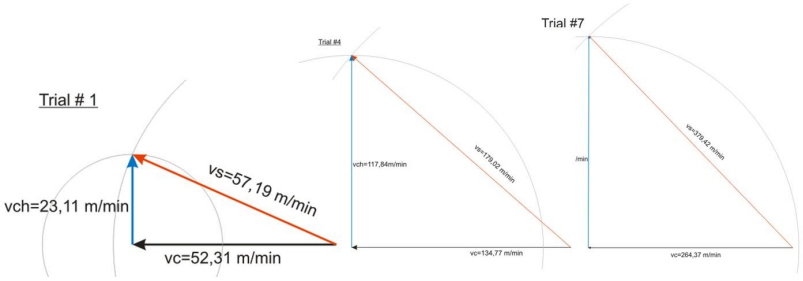


Figure 13 – The idealized velocity diagram according to Figure 12.

Table 2 presents the regular chips from the trials. No continuous or segmented strip, no helical profile. Only small and regular fragments with the mass description according to Figure 7. The irregular internal profile is impossible to be measured which helps the assumption of Figure 5. Based on production engineering point of view regarding the chip logistic, all the trials provided the same chip with a excellent packing factor.

Table 2 – The regular chip from the trials

| **Trial 1** | **Trial 2** | **Trial 3** | **Trial 4** |
|---|---|---|---|
| $v_c = 192{,}11\ \mathrm{m/min}$ | $v_c = 115{,}55\ \mathrm{m/min}$ | $v_c = 264{,}37\ \mathrm{m/min}$ | $v_c = 168{,}33\ \mathrm{m/min}$ |
| $\lambda_h = 1{,}01$ | $\lambda_h = 1{,}12$ | $\lambda_h = 0{,}97$ | $\lambda_h = 1{,}11$ |
| 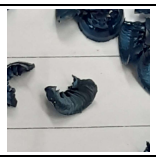 |  |  |  |

## 5. CONCLUSION

Even though this investigation is based on graduate classes of machining process it went further than regular topics because some concepts around the analysis are not based on theoretical principles but in a collection of experiments to support some assumptions. The assumption of not serrated chip is based on others experiments that indicates that chip volume theoretical definition is correct. The chip volume and mass are also correct because it was measured and the SAE 4340 for this investigation, applying this cutting tool exceeded on regularity of chip shape.

It is possible to affirm that chip formation was stable and about to be predicted not only by this classic theory but some other models newer than this one fully explained by Kronenberg (1966) and Shawn (1965).

Instead of using the Kronenberg's graphs (Figure 2) to obtain the shear angle, the practical definition base on chip compression factor proposed is enough to a very reasonable definition of a shear angle range.

Considering the unitary mass, the best chip was obtained with higher cutting speed. It converges with practical machining definition widespread.

The MRR should be the same according to Figure 11 and it is. However, a very important conclusion is taken when the MRR is the same and the chip velocity and the cutting speed are not the same. The flow frequency leans on the definition of a cycle or a set of cycles that result in a single chip. Furthermore the strain and strain rate play a role on the chip formation to explain the discontinuity throughout the shear strain theory around the shear plane. It justifies the difference between the values of cutting speed and chip velocity. But the continuity equation establishes that the mass remains the same amount even with the separation. So, it matters what happens in the machining system to produced the chip but the MRR can be defined from the continuity equation since the material removed is a measured amount regarding or not the velocity diagram.

## 6. REFERENCES

Astakhov, V.P., *Metal cutting mechanics*, CRC Press LLC, 1998, 297 p.

Astakhov, V.P., Osman, M.O.M., Hayajneh, M.T., Re-evaluation of the basic mechanics of metal cutting: Velocity diagram, virtual work equation and upper bound theorem, International Journal of Machine Tool and Manufacture, 41 (393-418), 2001

Kronenberg, M., *Machining Science and Application*, Pergamon Press, 1966, 410 p.

Merchant, M.E., Mechanics of the metal cutting Process.I. Orthogonal Cutting and a type 2 chip, Journal of applied physics, vol. 16, number 5, (267-275), 1945

Piispanen, Vaino, Theory of Formation of Metal Chips, Journal of applied Physics, 19, (876-881), 1948

Shaw, M.C. *Metal Cutting Principles,* 3rd Edition, The M.I.T Press, 1965, 472 p.

Stahl, J-E. *Metal Cutting Theories and Models*, Lund University, Sweden, 2012, 580 p.

Stephenson, D.A., Agapiou, J.S., *Metal Cutting Theory and Practice*, Third Edition, CRC Press, 2016, 956 p.

Tschätsch, H. *Applied Machining Technology*, Springer, 2009, 395 p.

Zorev, N.N., *Metal Cutting Mechanics*, Pergamon Press, 1966

## 7. RESPONSIBILITY NOTICE

The authors are the only responsible for the printed material included in this paper.